ELEKTROTEHNIŠKI VESTNIK 93(1-2): 32–43, 2026
ORIGINAL SCIENTIFIC PAPER

Optimization of the two-parameter seventh-order polynomial interpolation kernel in the spectral domain

Zoran Milivojević[1,†], Predrag Rajković[2]

[1]*The Academy of Applied Technical and Preschool Studies, Aleksandra Medvedeva 20, Niš, Serbia*
[2]*University of Niš, Faculty of Mechanical Engineering, Aleksandra Medvedeva 14, 18104 Niš, Serbia*

† *E-mail: zoran.milivojevic@akademijanis.edu.rs*

Abstract. The paper presents the optimization of a convolutional seventh-order two-parameter polynomial interpolation kernel. In its first part, the kernel is defined and its spectral characteristic $H(f)$ is determined using the Fourier transform. In the second part, the kernel optimization process in the spectral domain is described. The spectral characteristic is expanded into the Taylor series, and a flatness criterion is applied. A flatness criterion is used to prevent the upward and downward concavities of the spectral characteristic around $f = 0$, ensuring that it remains flat in this region. A flatness criterion is applied to minimize the ripple of the spectral characteristic in the pass-band. By optimizing the kernel, the optimal kernel parameters are $\alpha_{opt} = 241/28770$ and $\beta_{opt} = 13/77400$. The performance of the optimized kernel is evaluated in the spectral domain using similarity measures (error function $E(f)$, total square error E_T, and the slope of the spectral characteristic). The similarity is calculated with respect to the spectrum of the ideal interpolation kernel (box function). The similarity measures are presented in the tabular and graphical form. A direct comparison of the similarity measures demonstrates a higher similarity of the optimized seventh-order two-parameter kernel compared to the one-parameter kernel, with E_T reduced by the factor of 1.4866 and the slope k increased by the factor of 1.5209.

Keywords: convolution, interpolation, polynomial kernel, Fourier transform, Taylor series

Optimizacija dvo-parametrskega interpolacijskega jedra sedmega reda v spektralni domeni

Članek obravnava optimizacijo konvolucijskega interpolacijskega jedra sedmega reda z dvema parametroma. Najprej je jedro definirano in analizirano v spektralni domeni s Fourierovo transformacijo, nato pa je opisan postopek optimizacije. Spektralna karakteristika se razvije v Taylorjevo vrsto, pri čemer se uporabi kriterij ravnosti za zmanjšanje ukrivljenosti okoli $f = 0$ in valovanja v prepustnem pasu. Z optimizacijo dobimo optimalna parametra $\alpha_{opt} = 241/28770$ in $\beta_{opt} = 13/77400$. Učinkovitost optimiziranega jedra je ovrednotena v spektralni domeni z uporabo mer podobnosti (funkcija napake $E(f)$, skupna kvadratna napaka E_T in naklon spektralne karakteristike). Podobnost je izračunana glede na spekter idealnega interpolacijskega jedra (box funkcija). Mere podobnosti so predstavljene v tabelarični in grafični obliki. Neposredna primerjava mer podobnosti pokaže večjo podobnost optimiziranega dvoparametrskega jedra sedmega reda v primerjavi z enoparametrskim jedrom, pri čemer se E_T zmanjša za faktor 1.4866, naklon k pa poveča za faktor 1.5209.

Received 17 October 2025
Accepted 19 February 2026

1 INTRODUCTION

In digital signal processing (DSP), especially in image, audio and speech processing, there is a need to estimate the value of a discrete signal between two neighboring samples [1]. The numerical procedure for estimating the signal between two neighboring samples is called interpolation [2], [3]. In image processing, spatial transformations, rotations, geometric transformations, etc. are often performed [4], [5], [6]. When processing the speech signal, there is an intensive need to estimate the fundamental frequency when estimating the emotional and health status of the speaker, semantic and syntactic analysis of speech, speech synthesis, etc. [7].

The interpolation algorithms used in DSP, especially in real-time, are primarily required to have high precision and high execution speed [8]. Convolutional interpolation largely fulfills the mentioned requirements and that is why it is intensively implemented in DSP [9]. Convolutional interpolation is based on the application of interpolation kernel r. Interpolation is realized by convolution between a discrete signal (image, speech, audio signal,...) and a convolution kernel r [10]. The precision of the interpolation is directly dependent on the applied interpolation kernel. The ideal interpolation kernel has the form $\sin(x)/x$ and is denoted as sinc in the scientific literature [11]. In the time domain, the sinc kernel (r_{sinc}) is defined in the range $(-\infty, \infty)$. The spectral characteristic of the r_{sinc} kernel is a box characteristic (ideally flat in the pass-band and stop-band, and with an infinitely large slope in the transition band) [12]. A kernel with such defined characteristics is practically impossible to realize [13]. Through the process of windowization, it is possible to shorten the length of the r_{sinc} kernel by applying a box window function and, therefore, construct a $r_{\mathrm{sinc},w}$ kernel, which is used in convolutional interpolation. The spectral characteristic of the $r_{\mathrm{sinc},w}$ kernel has a significant ripple of the spectral characteristic in the pass-band and stop-band as well as a finite slope in the transition band. Therefore, the precision of the interpolation is unsatisfactory. A current problem in DSP is the construction of the interpolation kernel of finite length L_w and shape that satisfactorily approximates the r_{sinc} kernel in the time and spectral domain. The current approximation of the kernel is by means of low-order polynomials ($n \leq 7$).

Numerically, the simplest is the polynomial zeroth-order kernel ($n = 0$), where the interpolated value is determined by rounding to the nearest-neighbor sample. Convolution interpolation is realized very quickly, but the interpolation error is large. In recent decades, the linear (first-order, $n = 1$), the cubic (third-order, $n = 3$) [14], the quintic (fifth-order, $n = 5$), and the septic (seventh-order, $n = 7$) one-parameter (1P, α) interpolation kernels have been constructed [15], [16]. As the order n of the 1P kernels increases, the interpolation precision increases because the time-spectrum characteristics of the kernel are affected by changing the kernel parameter α. In this way, the optimization of the kernel parameter α is performed. In order to better adapt the kernel to the specific signal, two-parameter (2P, α, β) kernels were constructed. The third-order 2P kernel was first constructed, and later the fifth-order 2P kernel [17]. The construction of the seventh-order 2P kernel is presented in [18]. In [18] the spectral characteristic of the 2P kernel is not determined.

In this paper, the spectral characteristic, $H_{7th,2P}$, of the seventh-order 2P kernel, $r_{7th,2P}$, is determined, and the kernel is optimized in the spectral domain [18]. The optimization is performed according to the criterion that the spectral characteristic be flat around $f = 0$, which consequently leads to the minimization of the ripple of the spectral characteristic in the pass-band [16]. In the first part of the paper, the kernel $r_{7th,2P}$ is decomposed into the time components r_0, r_1, and r_2. Subsequently, the Fourier transform is applied to these kernel components, thereby determining the spectral characteristic of the kernel $H_{7th,2P}$. In the second part of the paper, the 2P kernel is optimized in the spectral domain according to the Flatness criterion [16]. The Flatness criterion ensures that the spectral characteristic is not concave upward nor concave downward around $f = 0$. Consequently, the ripple of the spectral characteristic $H_{7th,2P}$ is reduced, which in turn increases its similarity to the box spectral characteristic ($H_{\mathrm{sinc}} = H_{\mathrm{box}}$) of the ideal interpolation kernel r_{sinc}. Through the optimization process, the optimal values of the kernel parameters α_{opt} and β_{opt} are determined. In addition, optimization criteria in the time domain [13], [18] are applied: a) Slope criterion (equality of the slope of the time characteristic of the kernel with the slope of the r_{sinc} kernel at node $s = 1$), and b) Continuity criterion (continuity of the $(n-1)$th-order derivative at node $s = 1$). The performance of the following kernels is analyzed: a) non-parameterized kernels (nearest-neighbor, r_N, linear, r_L, and windowed, $r_{\mathrm{sinc},w}$), b) one-parameter (1P) kernels ($n = 3$, $n = 5$, $n = 7$), and c) the two-parameter (2P) kernel ($n = 7$) optimized in this paper, which are optimized according to the Slope, Continuity, and Flatness criteria. The performance is analyzed in the spectral domain using similarity measures: a) error function $E(f)$, b) total square error E_T, and c) slope of the spectral characteristic k [16]. The similarity measures are calculated with respect to the spectral characteristic H_{sinc} of the ideal interpolation kernel. All results are presented in tables and graphs. A detailed comparative analysis demonstrates the advantages of using the seventh-order 2P kernel.

The paper is further organized as follows. Section 2 describes the seventh-order 2P interpolation kernel. Section 3 describes the spectral characteristic of the 2P kernel. Section 4 describes the optimization in the spectral domain. Section 5 presents the performance of the optimized 2P kernel. Section 6 is Conclusion.

2 SEVENTH-ORDER INTERPOLATION 2P KERNEL

2.1 Definition of the 2P Kernel

In [16] the seventh-order polynomial 1P interpolation kernel is described. By extending this kernel and adding an additional kernel parameter, the seventh-order 2P kernel was constructed, as described in [17]. The 2P kernel is defined on the interval $(-5, 5)$ and approximates the ideal $\mathrm{sinc}(s)$ interpolation kernel. Outside this interval, the kernel is zero. The 2P kernel is composed of piecewise seventh-order polynomials, which are defined on the subintervals $(-5, -4)$, $(-4, -3)$, $(-3, -2)$, $(-2, -1)$, $(-1, 0)$, $(0, 1)$, $(1, 2)$, $(2, 3)$, $(3, 4)$, and $(4, 5)$. Therefore, the length of the kernel is $L_w = 10$. The kernel r is defined by:

$$r(s)=\begin{cases} a_{70}|s|^7+...+a_{10}|s|+a_{00}, & |s|\le 1\\ a_{71}|s|^7+...+a_{11}|s|+a_{01}, & 1<|s|\le 2\\ a_{72}|s|^7+...+a_{12}|s|+a_{02}, & 2<|s|\le 3\\ a_{73}|s|^7+...+a_{13}|s|+a_{03}, & 3<|s|\le 4\\ a_{74}|s|^7+...+a_{14}|s|+a_{04}, & 4<|s|\le 5\\ 0, & \text{otherwise}\end{cases}, \tag{1}$$

where the coefficients are $a_{70} = 245\alpha - 13909\beta + 821/1734$, $a_{60} = -621\alpha + 35289\beta - 1148/867$, $a_{50} = 0$, $a_{40} = 760\alpha - 43280\beta + 1960/867$ $a_{30} = 0$, $a_{20} = -384\alpha + 21900\beta - 1393/578$, $a_{10} = 0$, $a_{00} = 1$, $a_{71} = 301\alpha - 16855\beta + 1687/6936$, $a_{61} = -3309\alpha + 185593\beta - 2492/867$, $a_{51} = 14952\alpha - 839958\beta + 32683/2312$, $a_{41} = -35640\alpha + 2005060\beta - 6791/183$, $a_{31} = 47880\alpha - 2696750\beta + 2152/39$, $a_{21} = -36000\alpha + 2028996\beta - 13006/289$, $a_{11} = 14168\alpha - 798714\beta + 2413/139$, $a_{01} = -2352\alpha + 132628\beta - 2233/1156$, $a_{72} = 57\alpha - 2947\beta + 35/6936$, $a_{62} = -1083\alpha + 56295\beta - 175/1734$, $a_{52} = 8736\alpha - 456654\beta + 1995/2312$, $a_{42} = -38720\alpha + 2035660\beta - 4725/1156$, $a_{32} = 101640\alpha - 5374510\beta + 1575/136$, $a_{22} = -157632\alpha + 8382180\beta - 5670/289$, $a_{12} = 133336\alpha - 7127418\beta + 42525/2312$, $a_{02} = -47280\alpha + 2538900\beta - 8505/1156$, $a_{73} = \alpha$, $a_{63} = -27\alpha + 57\beta$, $a_{53} = 312\alpha - 1353\beta$, $a_{43} = -2000\alpha + 13360\beta$, $a_{33} = 7680\alpha - 70225\beta$, $a_{23} = -17664\alpha + 207174\beta$, $a_{13} = 22528\alpha - 325119\beta$, $a_{03} = -12288\alpha + 211932\beta$, $a_{74} = \beta$, $a_{64} = -34\beta$, $a_{54} = 495\beta$, $a_{44} = -4000\beta$, $a_{34} = 19375\beta$, $a_{24} = -56250\beta$, $a_{14} = 90625\beta$, and $a_{04} = -62500\beta$.

The values of the kernel parameters α and β directly affect: a) the time characteristics and b) the spectral characteristics of the 2P kernel, and consequently the interpolation precision. The interpolation precision is expressed through the interpolation error e and the mean square error (MSE). By minimizing the interpolation error, the optimal values of the kernel parameters α_{opt} and β_{opt} are determined, i.e., the 2P kernel is optimized. The optimization of the kernel can be performed in: a) the time domain, and b) the spectral domain.

2.2 Optimization of the 2P Kernel in the time domain

The optimization in the time domain is performed to increase the similarity of the 2P kernel r to the ideal interpolation kernel $\text{sinc}(s)$. In [17], the results of the time-domain optimization are presented, where the optimization criteria were: a) Slope criterion, and b) Continuity criterion [13]. According to the Slope criterion, the slope of the time characteristic of the 2P kernel $k_{7th,2P}$ at the nodes $s_k \in \{-1, 1\}$ should be equal to the slope of the $\text{sinc}(s)$ kernel, i.e., $k^t_{\text{sinc}}(s_k) = \frac{d}{ds}(\text{sinc}(s_k)) = \pm 1$. In this way, the optimal kernel parameters were determined as follows: for the 1P kernel, $\alpha_{\zeta,1P} = -1027/452574$, and for the 2P kernel, $\alpha_{\zeta,2P} = 146/1917$ and $\beta_{\zeta,2P} = 25/18257$.

Fig. 1.a shows the time characteristics of the ideal kernel r_{sinc}, the optimized 1P kernel $r_{\zeta,7th,1P}$, and the 2P kernel $r_{\zeta,7th,2P}$ according to the Slope criterion. According to the Continuity criterion, the continuity of the $(n-1)$th-order derivative of the time characteristic of the kernel r at the nodes $s_k \in \{-1, 1\}$ is required, which is ensured by $\lim_{s\to s_k^-} r^{(n-1)}(s) = \lim_{s\to s_k^+} r^{(n-1)}(s)$. Since the considered 2P kernel is of seventh-order ($n = 7$), the continuity condition applies to the sixth derivative, $\lim_{s\to s_k^-} r^{(6)}(s) = \lim_{s\to s_k^+} r^{(6)}(s)$. In this way, the optimal kernel parameters were determined as follows: for the 1P kernel, $\alpha_{\xi,1P} = -3133/2275008$ [13], and for the 2P kernel, $\alpha_{\xi,2P} = 145/4468$ and $\beta_{\xi,2P} = 30/50087$. Fig. 1.b shows the time characteristics of the ideal kernel r_{sinc}, the optimized 1P kernel $r_{\xi,7th,1P}$, and the 2P kernel $r_{\xi,7th,2P}$ according to the Continuity criterion.

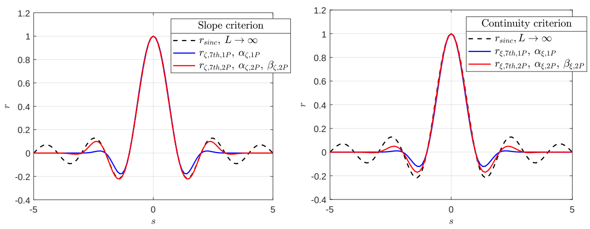

a) b)

Figure 1. Time characteristics of the kernels optimized according to: a) the Slope criterion (the ideal kernel r_{sinc}, the seventh-order 1P kernel $r_{\zeta,7th,1P}$ ($\alpha_{\zeta,1P} = -1027/452574$), and the seventh-order 2P kernel $r_{\zeta,7th,2P}$ ($\alpha_{\zeta,2P} = 146/1917$, $\beta_{\zeta,2P} = 25/18257$)); b) the Continuity criterion (the ideal kernel r_{sinc}, the seventh-order 1P kernel $r_{\xi,7th,1P}$ ($\alpha_{\xi,1P} = -3133/2275008$), and the seventh-order 2P kernel $r_{\xi,7th,2P}$ ($\alpha_{\xi,2P} = 145/4468$, $\beta_{\xi,2P} = 30/50087$)).

The following Section presents the determination of the spectral characteristic and, subsequently, the results of the 2P kernel optimization in the spectral-domain.

3 Spectral Characteristic of the 2P Kernel

The algorithm for determining the spectral characteristic of the seventh-order 2P kernel r (Eq. (1)) is realized in the following steps: a) decomposition of the kernel r into components r_0, r_1, and r_2; b) determination of the spectral characteristics of each kernel component H_0, H_1, and H_2; and c) determination of the spectral characteristic of the 2P kernel H.

3.1 Time components

The seventh-order 2P kernel (Eq. (1)) can be written in the form:

$$r(s) = r_0(s) + \alpha \cdot r_1(s) + \beta \cdot r_2(s), \tag{2}$$

where r_0, r_1, and r_2 are the kernel components. The component r_0 can be expressed in the form:

$$r_0(s) = \begin{cases} r_{0,0}(s), & |s| \le 1 \\ r_{0,1}(s), & 1 < |s| \le 2 \\ r_{0,2}(s), & 2 < |s| \le 3 \\ 0, & \text{otherwise} \end{cases}, \tag{3}$$

where

$$r_{0,0}(s) = \frac{821}{1734}|s|^7 - \frac{1148}{867}|s|^6 + 0|s|^5 + \frac{1960}{867}|s|^4 + 0|s|^3 - \frac{1393}{578}|s|^2, + 0|s| + 1 \tag{4}$$

$$r_{0,1}(s) = \frac{1687}{6936}|s|^7 - \frac{2492}{867}|s|^6 + \frac{32683}{2312}|s|^5 - \frac{128695}{3468}|s|^4 + \frac{127575}{2312}|s|^3 - \frac{13006}{289}|s|^2, + \frac{120407}{6936}|s| - \frac{2233}{1156} \tag{5}$$

and

$$r_{0,2}(s) = \frac{35}{6936}|s|^7 - \frac{175}{1734}|s|^6 + \frac{1995}{2312}|s|^5 - \frac{4725}{1156}|s|^4 + \frac{1575}{136}|s|^3 - \frac{5670}{289}|s|^2. + \frac{42525}{2312}|s| - \frac{8505}{1156} \tag{6}$$

The time kernel component r_1 can be written as:

$$r_1(s) = \begin{cases} r_{1,0}(s), & |s| \le 1 \\ r_{1,1}(s), & 1 < |s| \le 2 \\ r_{1,2}(s), & 2 < |s| \le 3 \\ r_{1,3}(s), & 3 < |s| \le 4 \\ 0, & \text{otherwise} \end{cases}, \tag{7}$$

where:

$$r_{1,0}(s) = 245|s|^7 - 621|s|^6 + 0|s|^5 + 760|s|^4 + 0|s|^3 - 384|s|^2 + 0|s| + 0, \tag{8}$$

$$r_{1,1}(s) = 301|s|^7 - 3309|s|^6 + 14952|s|^5 - 35640|s|^4 + 47880|s|^3 - 36000|s|^2, + 14168|s| - 2352 \tag{9}$$

$$r_{1,2}(s) = 57|s|^7 - 1083|s|^6 + 8736|s|^5 - 38720|s|^4 + 101640|s|^3 - 157632|s|^2, + 133336|s| - 47280 \tag{10}$$

and

$$r_{1,3}(s) = 1|s|^7 - 27|s|^6 + 312|s|^5 - 2000|s|^4 + 7680|s|^3 - 17664|s|^2 + 22528|s|. - 12288 \tag{11}$$

The time kernel component r_2 can be written as:

$$r_2(s) = \begin{cases} r_{2,0}(s), & |s| \le 1 \\ r_{2,1}(s), & 1 < |s| \le 2 \\ r_{2,2}(s), & 2 < |s| \le 3 \\ r_{2,3}(s), & 3 < |s| \le 4 \\ r_{2,4}(s), & 4 < |s| \le 5 \\ 0, & \text{otherwise} \end{cases}, \tag{12}$$

where:

$$r_{2,0}(s) = -13909|s|^7 + 35289|s|^6 + 0|s|^5 - 43280|s|^4 + 0|s|^3 + 21900|s|^2 + 0|s| + 0, \tag{13}$$

$$r_{2,1}(s) = -16855|s|^7 + 185593|s|^6 - 839958|s|^5 + 2005060|s|^4 - 2696750|s|^3 + 2028996|s|^2, - 798714|s| + 132628 \tag{14}$$

$$r_{2,2}(s) = -2947|s|^7 + 56295|s|^6 - 456654|s|^5 + 2035660|s|^4 - 5374510|s|^3 + 8382180|s|^2, - 7127418|s| + 2538900 \tag{15}$$

$$r_{2,3}(s) = 0|s|^7 + 57|s|^6 - 1353|s|^5 + 13360|s|^4 - 70225|s|^3 + 207174|s|^2, - 325119|s| + 211932 \tag{16}$$

and

$$r_{2,4}(s) = 1|s|^7 - 34|s|^6 + 495|s|^5 - 4000|s|^4 + 19375|s|^3. - 56250|s|^2 + 90625|s| - 62500 \tag{17}$$

The time forms of the kernel components of the 2P kernel are shown in Fig. 2: a) r_0 (Fig. 2.a), b) r_1 (Fig. 2.b), and c) r_2 (Fig. 2.c).

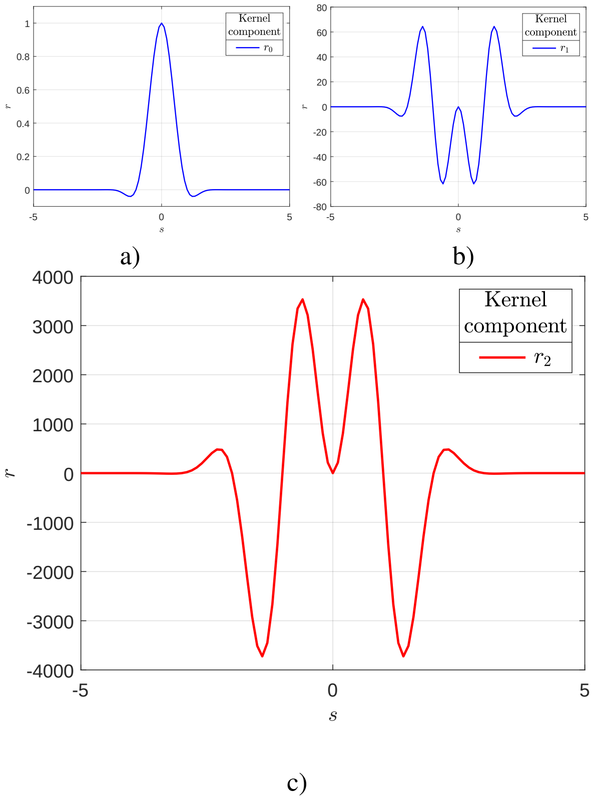

Figure 2. Time components of the 2P kernel: a) r_0, b) r_1, and c) r_2.

3.2 Spectral Components

The spectrum of the 2P kernel $H(f)$ is calculated by applying the Fourier transform:

$$\begin{aligned} H(f) &= \mathcal{F}\{r(s)\} \\ &= \mathcal{F}\{r_0(s) + \alpha r_1(s) + \beta r_2(s)\} \\ &= \mathcal{F}\{r_0(s)\} + \alpha\mathcal{F}\{r_1(s)\} + \beta\mathcal{F}\{r_2(s)\}, \\ &= H_0(f) + \alpha H_1(f) + \beta H_2(f) \end{aligned} \quad (18)$$

where H_0, H_1, and H_2 are the spectral components of the 2P kernel. The spectral component H_0 is:

$$H_0(f) = \int_{-\infty}^{\infty} r_0(s) e^{-i \cdot 2\pi s f} ds. \quad (19)$$

By substituting Eq. (3) into Eq. (19), the spectral components become:

$$H_0(f) = -\frac{1}{\pi^8 f^8} \begin{pmatrix} A\cos(2\pi f) \\ + B\cos(4\pi f) \\ + C\cos(6\pi f) \\ + D\sin(2\pi f) \\ + E\sin(4\pi f) \\ + F\cos(6\pi f) \\ - G \end{pmatrix}, \quad (20)$$

where:

$$A = \frac{267\pi^6 f^6}{81346268269379584} - \frac{899\pi^4 f^4}{162692536538759168} + \frac{167685}{18496}, \quad (21)$$

$$B = -\frac{1733\pi^6 f^6}{61009701202034688} + \frac{1879\pi^4 f^4}{162692536538759168} + \frac{43365}{4624}, \quad (22)$$

$$C = \frac{3675}{18496}\cos(6\pi f), \quad (23)$$

$$D = \frac{19\pi^7 f^7}{10168283533672448} - \frac{409\pi^5 f^5}{81346268269379584} + \frac{245\pi^3 f^3}{81346268269379584} + \frac{328965\pi f}{9248}, \quad (24)$$

$$E = -\frac{25\pi^7 f^7}{897201488265216} + \frac{899\pi^5 f^5}{40673134134689792} - \frac{245\pi^3 f^3}{81346268269379584} + \frac{14595\pi f}{2312}, \quad (25)$$

and

$$F = \frac{525\pi f}{9248}\sin(6\pi f) - \frac{86205}{4624}. \quad (26)$$

By eliminating coefficients with extremely small values (less than 10^{-14}), the spectral component H_0 is obtained:

$$H_0(f) = -\frac{1}{\pi^8 f^8} \begin{pmatrix} \frac{167685}{18496}\cos(2\pi f) \\ + \frac{43365}{4624}\cos(4\pi f) \\ + \frac{3675}{18496}\cos(6\pi f) \\ + \frac{328965}{9248}\pi f\sin(2\pi f) \\ + \frac{14595}{2312}\pi f\sin(4\pi f) \\ + \frac{525}{9248}\pi f\sin(6\pi f) \\ - \frac{86205}{4624} \end{pmatrix}. \quad (27)$$

The spectral component H_1 is:

$$H_1(f) = \int_{-\infty}^{\infty} r_1(s) e^{-i \cdot 2\pi s f} ds. \quad (28)$$

By substituting Eq. (7) into Eq. (28), the spectral component H_1 becomes:

$$H_1(f) = \frac{1}{\pi^8 f^8} \left(\begin{pmatrix} 36\pi^6 f^6 \\ -30\pi^4 f^4 \\ -1980\pi^2 f^2 \\ +\dfrac{17955}{8} \end{pmatrix} \cos(4\pi f) + \begin{pmatrix} \dfrac{1}{2}\pi^6 f^6 \\ -\dfrac{45}{4}\pi^4 f^4 \\ +\dfrac{225}{4}\pi^2 f^2 \\ -\dfrac{17955}{8} \end{pmatrix} \cos(6\pi f) + 96\pi^5 f^5 \sin(4\pi f) \right). \quad (29)$$

The spectral component H_2 is:

$$H_2(f) = \int_{-\infty}^{\infty} r_2(s) e^{-i \cdot 2\pi s f} ds. \quad (30)$$

By substituting Eq. (12) into Eq. (30), the spectral component H_2 becomes:

$$H_2(f) = \frac{1}{\pi^8 f^8} \begin{pmatrix} +8820\cos(2\pi f) \\ -3150\cos(4\pi f) \\ +105\cos(6\pi f) \\ +45\cos(8\pi f) \\ -427\sin(2\pi f) \\ +544\pi f\sin(2\pi f) \\ +297\pi f\sin(4\pi f) \\ +30\pi f\sin(6\pi f) \\ -4725 \end{pmatrix}. \quad (31)$$

The spectral components of the 2P kernel are shown in Fig. 3: a) H_0 (Fig. 3.a), b) H_1 (Fig. 3.b), and c) H_2 (Fig. 3.c).

3.3 Spectral characteristic of the 2P kernel

By substituting Eqs. (27), (29), and (31) into Eq. (18), the spectral characteristic of the seventh-order polynomial interpolation 2P kernel is determined. Fig. 4.a shows the spectral characteristics of the ideal interpolation kernel H_{sinc} and the windowed kernel $H_{\text{sinc,w}}$ of length $L_w = 10$, as well as the kernels optimized according to the Slope criterion: the 1P kernel $H_{\zeta,7th,1P}$ ($\alpha_{\zeta,1P} = -1027/452574$) and the 2P kernel $H_{\zeta,7th,2P}$ ($\alpha_{\zeta,2P} = 146/1917$, $\beta_{\zeta,2P} = 25/18257$). Fig. 4.b shows the spectral characteristics of the ideal interpolation kernel H_{sinc} and the windowed kernel $H_{\text{sinc,w}}$ of length $L_w = 10$, as well as the kernels optimized according to the Continuity criterion: the 1P kernel $H_{\xi,7th,1P}$ ($\alpha_{\xi,1P} = -3133/2275008$) and the 2P kernel $H_{\xi,7th,2P}$ ($\alpha_{\xi,2P} = 145/4468$, $\beta_{\xi,2P} = 30/50087$).

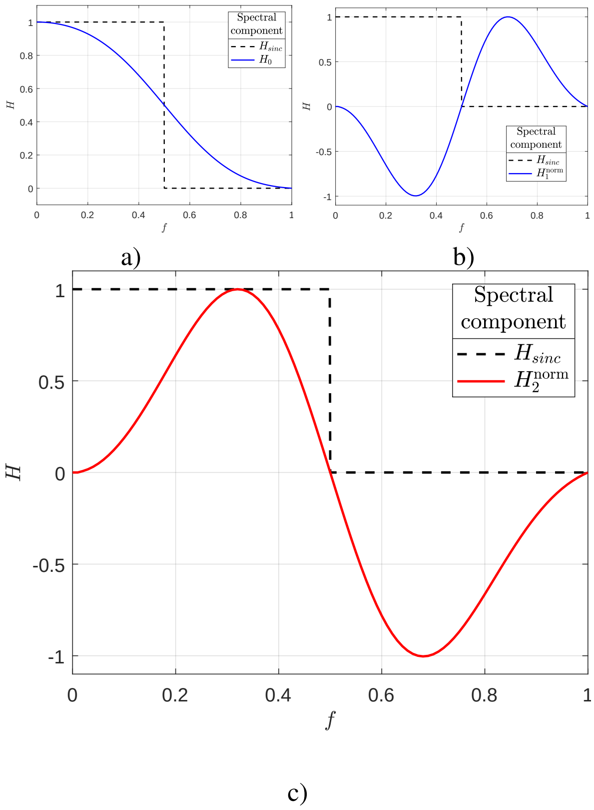

Figure 3. Spectral components of the 2P kernel: a) H_0, b) H_1, and c) H_2.

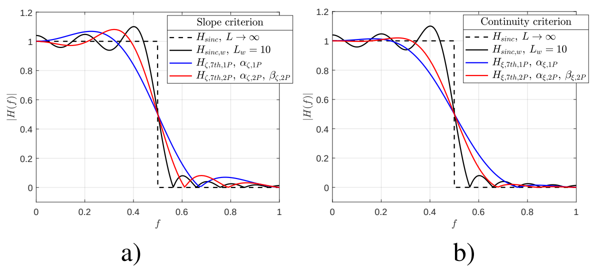

Figure 4. Spectral characteristics of the kernels optimized according to: a) the Slope criterion (ideal kernel r_{sinc}, seventh-order 1P kernel $r_{\zeta,7th,1P}$ ($\alpha_{\zeta,1P} = -1027/452574$), and seventh-order 2P kernel $r_{\zeta,7th,2P}$ ($\alpha_{\zeta,2P} = 146/1917$, $\beta_{\zeta,2P} = 25/18257$)); b) the Continuity criterion (ideal kernel r_{sinc}, seventh-order 1P kernel $r_{\xi,7th,1P}$ ($\alpha_{\xi,1P} = -3133/2275008$), and seventh-order 2P kernel $r_{\xi,7th,2P}$ ($\alpha_{\xi,2P} = 145/4468$, $\beta_{\xi,2P} = 30/50087$)).

4 Optimization in the Spectral Domain

Optimization in the time domain is performed with the aim of increasing the similarity of the spectral characteristic, H, of the seventh-order 2P kernel, r, to the spectral characteristic of the ideal interpolation kernel H_{sinc}. The spectral characteristic H_{sinc} has the following features: a) ideally flat $H_{\text{sinc}}(f) = 1$ in the pass-band, b) ideally flat $H_{\text{sinc}}(f) = 0$ in the stop-band, and c) a very large slope in the transition band ($k(1/2) \to \infty$). Due to the finite length L_w, the characteristics of interpolation kernels deviate from the ideal box characteristic (the ripple of the spectral characteristic exists in the pass-band and stop-band, and the slope in the transition band is finite). By varying the kernel parameters α and β, the shape of the spectral characteristic is directly affected. The optimization criterion is the minimization of the ripple in the spectral characteristic. To achieve this, conditions that the spectral characteristic must satisfy in the vicinity of $f = 0$ are imposed [16]. To prevent high-frequency emphasis, $H(f)$ must be convex downward, $\left.\frac{d^2H(f)}{df^2}\right|_{f=1/2} \leq 0$. To prevent low-frequency suppression, the spectral characteristic must be concave upward, $\left.\frac{d^2H(f)}{df^2}\right|_{f=1/2} \geq 0$. Both requirements are satisfied for:

$$\left.\frac{d^2H(f)}{df^2}\right|_{f=1/2} = 0. \tag{32}$$

This is the Flatness criterion, according to which the amplitude characteristic is flat in the vicinity of $f = 0$, which consequently results in the minimization of the ripple in the pass-band. During the optimization process, the optimal values of the kernel parameters α and β are determined in accordance with the Flatness criterion.

The Taylor series of the function $H(f)$ around $f_0 = 0$ (Maclaurin series) is:

$$\begin{aligned} T(f) =& \mathcal{T}(H(f) \\ &= \mathcal{T}(H_0(f) + \alpha H_1(f) + \beta H_2(f)) \\ &= \mathcal{T}(H_0(f)) + \alpha\mathcal{T}(H_1(f)) + \beta\mathcal{T}(H_2(f)), \\ &= T_0(f) + \alpha T_1(f) + \beta T_2(f) \end{aligned} \tag{33}$$

where T_0, T_1, and T_2 are the Taylor spectral components. By expanding up to the tenth-order, the Taylor spectral components are determined as follows:

$$\begin{aligned} T_0(f) =& 1 - \frac{142}{867}\pi^2 f^2 - \frac{137}{2719}\pi^4 f^4 \\ &+ \frac{95}{4672}\pi^6 f^6 - \frac{41}{13143}\pi^8 f^8 + O(f^{10}) \end{aligned}, \tag{34}$$

$$\begin{aligned} T_1(f) =& -192\pi^2 f^2 + \frac{1024}{11}\pi^4 f^4 \\ &+ \frac{13991}{482}\pi^6 f^6 - \frac{5353}{179}\pi^8 f^8 + O(f^{10}) \end{aligned}, \tag{35}$$

and

$$\begin{aligned} T_2(f) =& 10560\pi^2 f^2 - 4352\pi^4 f^4 \\ &- \frac{28923}{13}\pi^6 f^6 + \frac{21930}{13}\pi^8 f^8 + O(f^{10}) \end{aligned}. \tag{36}$$

By substituting Eqs. (34), (35), and (36) into Eq. (33), the Taylor series of the spectral characteristic is obtained:

$$\begin{aligned} T =& T_0 + \alpha \cdot T_1 + \beta \cdot T_2 = \\ & 1 + \left(-\frac{142}{867} - 192\alpha + 10560\beta\right)\pi^2 f^2 \\ &+ \left(-\frac{137}{2719} + \frac{1024}{11}\alpha - 4352\beta\right)\pi^4 f^4 \\ &+ \left(\frac{95}{4672} + \frac{13991}{482}\alpha - \frac{28923}{13}\beta\right)\pi^6 f^6 \\ &+ \left(-\frac{41}{13143} - \frac{5353}{179}\alpha + \frac{21930}{13}\beta\right)\pi^8 f^8 \\ &+ O(f^{10}) \end{aligned}. \tag{37}$$

In accordance with the Flatness criterion, in order to ensure that the spectral characteristic, $H(f)$, is flat in the vicinity of $f = 0$ i.e., without ripple, it is required that the coefficient of the f^2 term in the Taylor series be equal to zero: $\implies -142/867 - 192\alpha + 10560 = 0$. This equation contains two unknowns, α and β, and therefore does not have a unique solution. For this reason, a stricter condition is introduced, namely that the coefficient of the f^4 term is also equal to zero: $\implies -137/2719 + 1024/11\alpha - 4352\beta = 0$. From these two equations, a system of two equations with two unknowns is formed:

$$\begin{cases} -\frac{142}{867} - 192\alpha + 10560\beta = 0 \\ -\frac{137}{2719} + \frac{1024}{11}\alpha - 4352\beta = 0 \end{cases}. \tag{38}$$

By solving the system, the values of the parameters that are optimal in accordance with the Flatness criterion are obtained:

$$\alpha_{opt} = \alpha_\omega = \frac{241}{28770}, \quad \beta_{opt} = \beta_\omega = \frac{13}{77400}.$$

Figure 5.a shows the time-domain characteristics of the ideal kernel, r_{sinc}, and the kernels optimized according to the Flatness criterion: a) seventh-order 1P kernel $r_{\omega,7th,1P}$ ($\alpha_{\omega,1P} = -71/83232$), and b) seventh-order 2P kernel $r_{\omega,7th,2P}$ ($\alpha_{\omega,2P} = 241/28770$, $\beta_{\omega,2P} = 13/77400$). Figure 5.b shows the spectral characteristics of the ideal kernel, H_{sinc}, the windowed kernel $H_{\text{sinc,w}}$ of length $L_w = 10$, and the kernels optimized according to the Flatness criterion: a) seventh-order 1P kernel $H_{\omega,7th,1P}$ ($\alpha_{\omega,1P}$) [16], and b) seventh-order 2P kernel $H_{\omega,7th,2P}$ ($\alpha_{\omega,2P}$, $\beta_{\omega,2P}$).

5 Performance of the Optimized 2P Kernel

The spectral characteristics of the kernels, H, which are optimized according to: a) the Slope criterion: i) $H_{\zeta,3rd,1P}$, ii) $H_{\zeta,5th,1P}$, iii) $H_{\zeta,7th,1P}$, and iv) $H_{\zeta,7th,2P}$ (Fig. 4.a); b) the Continuity criterion: i)

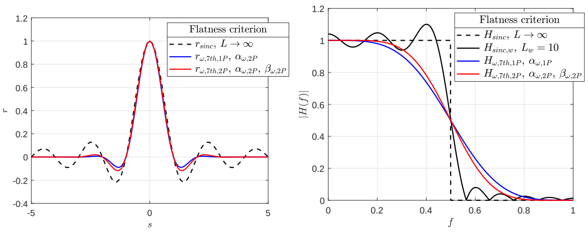

a) b)

Figure 5. a) Time-domain characteristics of the ideal kernel r_{sinc} and the kernels optimized according to the Flatness criterion: i) seventh-order 1P kernel $r_{\omega,7th,1P}$ ($\alpha_{\omega,1P} = -71/83232$), and ii) seventh-order 2P kernel $r_{\omega,7th,2P}$ ($\alpha_{\omega,2P} = 241/28770$, $\beta_{\omega,2P} = 13/77400$); b) Spectral characteristics of the ideal kernel H_{sinc}, the windowed kernel $H_{\text{sinc,w}}$ of length $L_w = 10$, and the kernels optimized according to the Flatness criterion: i) seventh-order 1P kernel $H_{\omega,7th,1P}$ ($\alpha_{\omega,1P}$), and ii) seventh-order 2P kernel $H_{\omega,7th,2P}$ ($\alpha_{\omega,2P}$, $\beta_{\omega,2P}$).

$H_{\xi,3rd,1P}$, ii) $H_{\xi,5th,1P}$, iii) $H_{\xi,7th,1P}$, and iv) $H_{\xi,7th,2P}$ (Fig. 4.b); and c) the Flatness criterion: i) $H_{\omega,3rd,1P}$, ii) $H_{\omega,5th,1P}$, iii) $H_{\omega,7th,1P}$, and iv) $H_{\omega,7th,2P}$ (Fig. 5.b), are compared with the spectral characteristic of the ideal kernel H_{sinc}, which has the form of a box function. In addition, the spectral characteristics of the non-parameterized kernels: the windowed $H_{\text{sinc,w}}$, and the polynomial kernels of zero-degree (nearest-neighbor interpolation) H_N, and first-degree (linear interpolation) H_L, are compared.

5.1 Similarity measures

As a measure of the deviation of the spectral characteristics of the kernels from the box characteristic, the following similarity measures were used: a) the error function $E(f)$, b) the total square error E_T, and c) the slope $k(1/2)$ (the slope of the spectral characteristic in the transition range between the pass-band ($0 < f \leq 1/2$) and the stop-band ($1/2 < f$)).

The error function, $E(f)$, represents the squared difference of the spectral characteristics and is defined as:

$$E(f) = |1 - H(f)|^2 . \tag{39}$$

The total square error, E_T, is defined as the integral of the squared difference of the spectral characteristics over the pass-band frequency range:

$$E_T = \int_{-1}^{1} |1 - H(f)|^2 \, df = \int_{-1/2}^{1/2} E(f) \, df. \tag{40}$$

The slope of the spectral characteristic, k, is defined as the derivative of the spectral characteristic (Eq. (18)) in the transition band, evaluated at $f = 1/2$:

$$k = \left. \frac{dH(f)}{df} \right|_{f=1/2} . \tag{41}$$

Finally, the slope of the seventh-order 2P kernel optimized according to the Flatness criterion is:

$$k_{\omega,7th,2P} = -\frac{647}{351} + \alpha\frac{31778}{39} - \beta 48074. \tag{42}$$

5.2 Results

In Fig. 6.a, the error function, $E(f)$, is shown for the seventh-order polynomial 1P and 2P kernels, optimized according to: a) the Slope criterion ($E_{\zeta,7th,1P}$, $E_{\zeta,7th,2P}$), b) the Continuity criterion ($E_{\xi,7th,1P}$, $E_{\xi,7th,2P}$), and c) the Flatness criterion ($E_{\omega,7th,1P}$, $\alpha_{\omega,1P}$, $E_{\omega,7th,2P}$). In Fig. 6.b, the corresponding error functions are presented as log-plots. In Table 1, the results of the total square error E_T and the slope of the spectral characteristic $k(-1/2)$ are presented for all analyzed interpolation kernels.

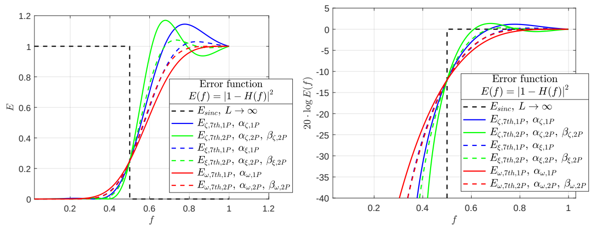

a) b)

Figure 6. *a*) The error function, $E(f)$, for the seventh-order polynomial 1P and 2P kernels: i) the Slope criterion ($E_{\zeta,7th,1P}$, $E_{\zeta,7th,2P}$), ii) the Continuity criterion ($E_{\xi,7th,1P}$, $E_{\xi,7th,2P}$), and iii) the Flatness criterion ($E_{\omega,7th,1P}$, $\alpha_{\omega,1P}$, $E_{\omega,7th,2P}$); *b*) Log-plots of the corresponding error functions.

For the purpose of a comparative analysis of the execution time, t_{exe}, of all tested kernels, the execution time was measured using the MATLAB functions `tic` and `toc`. The measurement was performed on the test platform: computer DESKTOP-S2AC43P, processor: Intel(R) Pentium(R) CPU G3220 3 GHz, RAM: 8 GB, Windows 10 operating system. The execution time, $\bar{t}$, was calculated as the arithmetic mean over 10 million measurements, while, t_{min}, was determined as the minimum value among all measurements. The execution times of the tested interpolation kernels are: $\bar{t}_{r_{\text{sinc},w}} = 2.2260\,\mu s$, $t_{r_{\text{sinc},w},min} = 1.9863\,\mu s$, $\bar{t}_{r_N} = 0.19682\,\mu s$, $t_{r_N,min} = 0.1\,\mu s$, $\bar{t}_{r_L} = 0.19959\,\mu s$, $t_{r_L,min} = 0.1\,\mu s$, $\bar{t}_{r_{3rd,1P}} = 0.36574\,\mu s$, $t_{r_{3rd,1P},min} = 0.3\,\mu s$, $\bar{t}_{r_{5th,1P}} = 0.67613\,\mu s$, $t_{r_{5th,1P},min} = 0.5\,\mu s$, $\bar{t}_{r_{7th,1P}} = 0.99561\,\mu s$, $t_{r_{7th,1P},min} = 0.8\,\mu s$, and $\bar{t}_{r_{7th,2P}} = 0.9995\,\mu s$, $t_{r_{7th,2P},min} = 0.8\,\mu s$. In Fig. 7 the execution times of the interpolation kernels are presented graphically.

5.3 Results analysis

Based on the results shown in Table 1, it can be concluded that, for the applied Slope criterion for parameter optimization (equalizing the slope of the kernel's

Table 1. Total square error E_T and slope $k(1/2)$.

Kernel	α	β	E_T	$k(-1/2)$
r_{sinc}	-	-	0	∞
$r_{\text{sinc},w}$	-	-	0.0201	9.9916
r_N	-	-	0.1280	1.5985
r_L	-	-	0.1169	1.6202
Slope criterion				
Kernel	α_ζ	β_ζ	$E_{T,\zeta}$	$k_\zeta(-1/2)$
$r_{3rd,1P}$	-1	0	0.0580	3.1312
$r_{5th,1P}$	11/96	0	0.0532	3.4862
$r_{7th,1P}$	-1027/452574	0	0.0501	3.6923
$r_{7th,2P}$	146/1917	25/18257	0.0337	5.6156
Continuity criterion				
Kernel	α_ξ	β_ξ	$E_{T,\xi}$	$k_\xi(-1/2)$
$r_{3rd,1P}$	-3/4	0	0.0660	2.7260
$r_{5th,1P}$	1/13	0	0.0623	2.8924
$r_{7th,1P}$	-3133/2275008	0	0.0609	2.9654
$r_{7th,2P}$	145/4468	30/50087	0.0428	4.1942
Flatness criterion				
Kernel	α_ω	β_ω	$E_{T,\omega}$	$k_\omega(-1/2)$
$r_{3rd,1P}$	-1/2	0	0.0788	2.3207
$r_{5th,1P}$	3/64	0	0.0758	2.4186
$r_{7th,1P}$	-71/83232	0	0.0723	2.5384
$r_{7th,2P}$	241/28770	13/77400	0.0595	3.0922

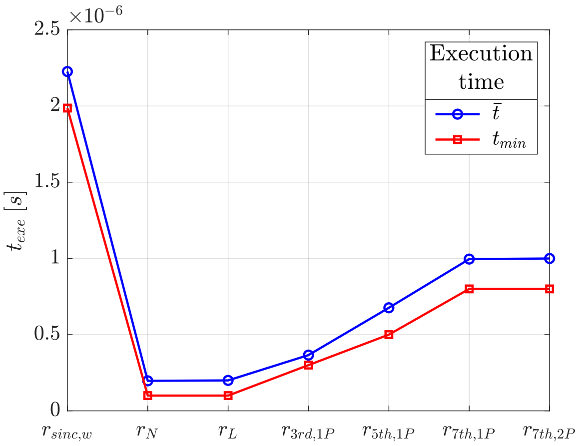

Figure 7. a) The mean execution time, $\bar{t}$, and b) the minimum execution time, t_{min}, of the interpolation kernels.

time characteristic with the slope of the sinc kernel at the node $s = 1$), the total square error, E_T, of the seventh-order polynomial 2P kernel $r_{\zeta,7th,2P}$ is smaller compared to:

a) Non-parameterized polynomial kernels: i) nearest-neighbor $(r_N, n = 0) \Rightarrow E_{T,N}/E_{T\zeta,7th,2P} = 0.1280/0.0337 = 3.7982$, and ii) linear $(r_L, n = 1) \Rightarrow E_{T,L}/E_{T\zeta,7th,2P} = 0.1169/0.0337 = 3.4688$ times; b) Parameterized 1P kernels: i) $(r_{3rd,1P}, n = 3) \Rightarrow E_{T\zeta,3rd,1P}/E_{T\zeta,7th,2P} = 0.0580/0.0337 = 1.7211$, ii) $(r_{5th,1P}, n = 5) \Rightarrow E_{T\zeta,5th,1P}/E_{T\zeta,7th,2P} = 0.0532/0.0337 = 1.5786$, and iii) $(r_{7th,1P}, n = 7) \Rightarrow E_{T\zeta,7th,1P}/E_{T\zeta,7th,2P} = 0.0501/0.0337 = 1.4866$ times; and c) Windowed sinc kernel $(r_{\text{sinc},w}) \Rightarrow E_{T,\text{sinc},w}/E_{T\zeta,7th,2P} = 0.0201/0.0337 = 0.5964$ times.

The Total square error E_T for the 2P kernel optimized according to the Continuity criterion is smaller compared to: a) Non-parameterized polynomial kernels: i) nearest-neighbor $(r_N, n = 0) \Rightarrow E_{T,N}/E_{T\xi,7th,2P} = 0.1280/0.0428 = 2.9907$, and ii) linear $(r_L, n = 1) \Rightarrow E_{T,L}/E_{T\xi,7th,2P} = 0.1169/0.0428 = 2.7313$ times; b) Parameterized 1P kernels: i) $(r_{3rd,1P}, n = 3) \Rightarrow E_{T\xi,3rd,1P}/E_{T\xi,7th,2P} = 0.0660/0.0428 = 1.5421$, ii) $(r_{5th,1P}, n = 5) \Rightarrow E_{T\xi,5th,1P}/E_{T\xi,7th,2P} = 0.0623/0.0428 = 1.4556$, and iii) $(r_{7th,1P}, n = 7) \Rightarrow E_{T\xi,7th,1P}/E_{T\xi,7th,2P} = 0.0609/0.0428 = 1.4229$ times; and c) Windowed sinc kernel $(r_{\text{sinc},w}) \Rightarrow E_{T,\text{sinc},w}/E_{T\xi,7th,2P} = 0.0201/0.0428 = 0.4696$ times.

The total square error, E_T, for the 2P kernel optimized according to the Flatness criterion is smaller compared to: a) Non-parameterized polynomial kernels: i) nearest-neighbor $(r_N, n = 0) \Rightarrow E_{T,N}/E_{T\omega,7th,2P} =$

$0.1280/0.0595 = 2.1513$, and ii) linear $(r_L, n = 1) \Rightarrow E_{T,L}/E_{T\omega,7th,2P} = 0.1169/0.0595 = 1.9647$ times; b) Parameterized 1P kernels: i) $(r_{3rd,1P}, n = 3) \Rightarrow E_{T\omega,3rd,1P}/E_{T\omega,7th,2P} = 0.0788/0.0595 = 1.3244$, ii) $(r_{5th,1P}, n = 5) \Rightarrow E_{T\omega,5th,1P}/E_{T\omega,7th,2P} = 0.0758/0.0595 = 1.2739$, and iii) $(r_{7th,1P}, n = 7) \Rightarrow E_{T\omega,7th,1P}/E_{T\omega,7th,2P} = 0.0723/0.0595 = 1.2151$ times; and c) Windowed sinc $(r_{\text{sinc},w}) \Rightarrow E_{T,\text{sinc},w}/E_{T\omega,7th,2P} = 0.0201/0.0595 = 0.3378$ times.

The total square error, E_T, for the seventh-order 2P kernel optimized according to the Flatness criterion is larger compared to: a) the Slope criterion: $E_{T\omega,7th,2P}/E_{T\zeta,7th,2P} = 0.0595/0.0337 = 1.8030$, and b) the Continuity criterion: $E_{T\omega,7th,2P}/E_{T\xi,7th,2P} = 0.0595/0.0428 = 1.4167$ times.

The slope of the spectral characteristic of the seventh-order 2P polynomial kernel, optimized according to the Slope criterion, in the transition band $k(1/2)$, is larger compared to: a) Non-parameterized polynomial kernels: i) nearest-neighbor $(r_N, n = 0) \Rightarrow k_{\zeta,7th,2P}/k_N = 5.6156/1.5985 = 3.5130$, and ii) linear $(r_L, n = 1) \Rightarrow k_{\zeta,7th,2P}/k_L = 5.6156/1.6202 = 3.4660$ times; b) Parameterized 1P kernels: i) $(r_{3rd,1P}, n = 3) \Rightarrow k_{\zeta,7th,2P}/k_{\zeta,3rd,1P} = 5.6156/3.1312 = 1.7934$, ii) $(r_{5th,1P}, n = 5) \Rightarrow k_{\zeta,7th,2P}/k_{\zeta,5th,1P} = 5.6156/3.4862 = 1.6108$, and iii) $(r_{7th,1P}, n = 7) \Rightarrow k_{\zeta,7th,2P}/k_{\zeta,7th,1P} = 5.6156/3.6923 = 1.5209$ times; and c) Windowed sinc $(r_{\text{sinc},w}) \Rightarrow k_{\zeta,7th,2P}/k_{\text{sinc},w} = 5.6156/9.9916 = 0.5620$ times.

The slope, $k(1/2)$, for the 2P kernel optimized according to the Continuity criterion is larger compared to: a) Non-parameterized polynomial kernels: i) nearest-neighbor $(r_N, n = 0) \Rightarrow k_{\xi,7th,2P}/k_N = 4.1942/1.5985 = 2.6238$, and ii) linear $(r_L, n = 1) \Rightarrow k_{\xi,7th,2P}/k_L = 4.1942/1.6202 = 2.5887$ times; b) Parameterized 1P kernels: i) $(r_{3rd,1P}, n = 3) \Rightarrow k_{\xi,7th,2P}/k_{\xi,3rd,1P} = 4.1942/2.7260 = 1.5386$, ii) $(r_{5th,1P}, n = 5) \Rightarrow k_{\xi,7th,2P}/k_{\xi,5th,1P} = 4.1942/2.8924 = 1.4501$, and iii) $(r_{7th,1P}, n = 7) \Rightarrow k_{\xi,7th,2P}/k_{\xi,7th,1P} = 4.1942/2.9654 = 1.4144$ times; and c) Windowed sinc $(r_{\text{sinc},w}) \Rightarrow k_{\xi,7th,2P}/k_{\text{sinc},w} = 4.1942/9.9916 = 0.4198$ times.

The slope, $k(1/2)$, for the 2P kernel optimized according to the Flatness criterion is smaller compared to: a) Non-parameterized polynomial kernels: i) nearest-neighbor $(r_N, n = 0) \Rightarrow k_{\omega,7th,2P}/k_N = 3.0922/1.5985 = 1.9344$, and ii) linear $(r_L, n = 1) \Rightarrow k_{\omega,7th,2P}/k_L = 3.0922/1.6202 = 1.9085$ times; b) Parameterized 1P kernels: i) $(r_{3rd,1P}, n = 3) \Rightarrow k_{\omega,7th,2P}/k_{\omega,3rd,1P} = 3.0922/2.3207 = 1.3324$, ii) $(r_{5th,1P}, n = 5) \Rightarrow k_{\omega,7th,2P}/k_{\omega,5th,1P} = 3.0922/2.4186 = 1.2785$, and iii) $(r_{7th,1P}, n = 7) \Rightarrow k_{\omega,7th,2P}/k_{\omega,7th,1P} = 3.0922/2.5384 = 1.2182$ times; and c) Windowed sinc $(r_{\text{sinc},w}) \Rightarrow k_{\omega,7th,2P}/k_{\text{sinc},w} = 3.0922/9.9916 = 0.3095$ times.

The slope, $k(1/2)$, for the seventh-order 2P kernel optimized according to the Flatness criterion is smaller compared to: a) the Slope criterion: $k_{\zeta,7th,2P}/k_{\omega,7th,2P} = 5.6156/3.0922 = 1.8161$, and b) the Continuity criterion: $k_{\xi,7th,2P}/k_{\omega,7th,2P} = 4.1942/3.0922 = 1.3564$ times.

Based on the execution times and Fig. 7, it can be concluded that the smallest execution times are for the nearest-neighbor and linear kernels ($t_{min} = 100\,ns$), and that with increasing kernel order, the execution times increase ($n = 3 \Rightarrow t_{min} = 300\,ns$, $n = 5 \Rightarrow t_{min} = 500\,ns$, and $n = 7 \Rightarrow t_{min} = 800\,ns$). The largest execution time is observed for the windowed $r_{\text{sinc},w}$ kernel $\Rightarrow t_{min} = 1.9863\mu s$. The execution times of the seventh-order 1P and 2P kernels are identical ($t_{min} = 800\,ns$). However, for real-time interpolation, the convolution algorithm must be implemented in a programming language (e.g., C), where compiler optimizations can reduce the program execution time.

Based on the detailed comparative analysis, it can be concluded that the seventh-order polynomial 2P kernel ($r_{7th,2P}$), optimized according to the Slope, Continuity, and Flatness criteria, has, compared to the windowed sinc kernel ($r_{\text{sinc},w}$), the non-parameterized kernels (r_N, r_L), and the parameterized 1P kernels ($r_{3rd,1P}$, $r_{5th,1P}$, $r_{7th,1P}$): a) a smaller total square error, E_T, and b) a larger slope, $k(1/2)$, in accordance with the corresponding optimization criteria. In a direct comparison of the seventh-order polynomial 1P ($r_{7th,1P}$) and 2P ($r_{7th,2P}$) interpolation kernels, it is observed that the 2P kernel has a smaller E_T by 1.4866, 1.4229, and 1.2151 times, and a larger slope by 1.5209, 1.4144, and 1.2182 times. Furthermore, the execution times for the 1P and 2P kernels are identical ($t_{min} = 100\,ns$). Taking into account: a) the previously presented comparative analysis and b) the execution time, the seventh-order 2P interpolation kernel, with parameters $\alpha_{opt} = 241/28770$ and $\beta_{opt} = 13/77400$, can be recommended for implementation in real-time systems.

6 Conclusion

This paper has presented the optimization of the seventh-order polynomial convolutional interpolation two-parameter kernel r. The optimization was performed in the spectral domain, on the spectral characteristic H, which was determined by applying the Fourier transform. The optimization was carried out by applying the Flatness criterion, according to which the spectral characteristic of the kernel in the vicinity of $f = 0$ exhibits neither upward nor downward concavity, i.e., it remains flat. In this way, the ripple of the spectral characteristic was minimized. For the purpose of minimizing the spectral characteristic, it was expanded into a Taylor series around $f = 0$ (McLaren series). The elimination of concavity and the minimization of the ripple of the spectral characteristic were achieved by removing the terms of the Taylor series that predominantly contribute to the ripple. In this way, the optimization of the kernel (r_{opt}, H_{opt}) was carried out, and the optimal values of the kernel parameters were determined as $\alpha = 241/28770$ and $\beta = 13/77400$. The validation of the optimization effect in the spectral domain was performed by calculating the similarity between the spectral characteristic, H_{opt}, and the spectral characteristic of the ideal interpolation kernel, H_{sinc}. The similarity measures used were the error function, $E(f)$, the total square error, E_T, and the slope, $k(1/2)$. The similarity measures were calculated for the windowed sinc kernel ($r_{\mathrm{sinc},w}$), the non-parameterized polynomial kernels (zero-order, first-order), and the parameterized 1P kernels (third-order, fifth-order, and seventh-order). For all kernels, in addition to the spectral domain optimization according to the Flatness criterion, the similarity measures were also determined for the optimization in the time domain (Slope criterion, Continuity criterion). A detailed comparative analysis showed that the optimized seventh-order 2P kernel, compared to the optimized seventh-order 1P kernel, has a smaller E_T by 1.4866 (Slope criterion), 1.4229 (Continuity criterion), and 1.2151 (Flatness criterion) times, and a higher slope of the spectral characteristic $k(1/2)$ by 0.5620 (Slope criterion), 1.5386 (Continuity criterion), and 1.2182 (Flatness criterion) times. The execution time of the 2P kernel is equal to that of the 1P kernel ($t = 800$ ns). Considering the results of the comparative analysis, the seventh-order polynomial 2P kernel with parameters $\alpha_{opt} = 241/28770$ and $\beta_{opt} = 13/77400$ can be recommended for use in real-time systems.

Data Availability

The numerical data used to generate the figures in this paper have been made openly available at Zenodo: https://doi.org/10.5281/zenodo.18421676.

References

[1] A. Carson, V. Valimaki, A. Wright, and S. Bilbao, Resampling filter design for multirate neural audio effect processing, *IEEE Transactions on Audio, Speech and Language Processing*, Vol. 33, pp. 2163–2174, 2025.

[2] A. Kazuyuki, K. Shoichi, and S. Hiroshi, Spatial active noise control based on individual kernel interpolation of primary and secondary sound fields, in *IEEE International Conference on Acoustics, Speech and Signal Processing (ICASSP)*, Singapore, pp. 1056–1060, 2022.

[3] R. Sikora, P. Markiewicz, M. Maczka, and S. Pawlowski, Using interpolation method to estimation step and touch voltage in grounding system, *Przeglad Elektrotechniczny*, Vol. 99, No. 2, pp. 263–266, 2023.

[4] K. K. Delibasis, I. P. Oikonomou, A. I. Kechriniotis, and G. N. Tsigaridas, Hermite coordinate interpolation kernels: application to image zooming, *ArXiv*, Vol. abs/2403.13195, 2024.

[5] B. Sun and S. Xin, An edge-guided weighted image interpolation algorithm, in *2023 IEEE 13th International Conference on Electronics Information and Emergency Communication (ICEIEC)*, Beijing, China, pp. 139–143, 2023.

[6] O. Rukundo and B. Maharaj, Optimization of image interpolation based on nearest neighbor algorithm, in *International Conference on Computer Vision Theory and Applications (VISAPP)*, Lisbon, Portugal, pp. 641–647, 2014.

[7] G. Zilu, W. Qing, D. Jun, P. Jia, L. Qing, and L. Chin, A variance-preserving interpolation approach for diffusion models with applications to single channel speech enhancement and recognition, *IEEE/ACM Transactions on Audio, Speech, and Language Processing*, Vol. 32, pp. 3025–3038, 2024.

[8] H. Kim, J. Kim, and S. Lee, Accelerating the computation for real-time application of the sinc function using GPUs, *Journal of Analytical Science and Technology*, vol. 11, no. 8, 2020.

[9] M. Maczka, S. Pawlowski, and G. Haldas, Application of polynomial approximation in simulations of quantum cascade lasers, *Przeglad Elektrotechniczny*, Vol. 98, No. 12, pp. 321–324, 2022.

[10] E. Meijering, A chronology of interpolation: From ancient astronomy to modern signal and image processing, *Proceedings of the IEEE*, Vol. 90, No. 3, pp. 319–342, 2002.

[11] L. P. Yaroslavsky, Fast discrete sinc-interpolation: A gold standard for image resampling, in *Image Processing: Algorithms and Systems*, Springer, 2014, pp. 3–16.

[12] S. Maymon and A. V. Oppenheim, Sinc interpolation of nonuniform samples, *IEEE Transactions on Signal Processing*, Vol. 59, No. 10, pp. 4745–4758, Oct. 2011.

[13] E. Meijering, J. Niessen, J. Pluim, and M. Viergever, Quantitative comparison of sinc-approximating kernels for medical image interpolation, in *Lecture Notes in Computer Science*, pp. 210–217, 2000.

[14] R. Keys, Cubic convolution interpolation for digital image processing, *IEEE Transactions on Acoustics, Speech, and Signal Processing*, Vol. 29, No. 1, pp. 1153–1160, 1981.

[15] E. Meijering and M. Unser, A note on cubic convolution interpolation, *IEEE Transactions on Image Processing*, Vol. 12, No. 4, pp. 477–479, 2003.

[16] K. Meijering, M. Zuiderveld, and A. Viegever, Image reconstruction by convolution with symmetrical piecewise n-th-order polynomial kernels, *IEEE Transactions on Image Processing*, Vol. 8, No. 2, pp. 192–201, 1999.

[17] Z. Milivojević and R. Ivković, Optimization of the polynomial fifth-order interpolation 2P kernel in the time-domain, *Elektrotehniški Vestnik (Electrotechnical Review)*, Vol. 91, No. 5, pp. 247–256, 2024.

[18] Z. Milivojević, N. Savić, B. Prlinčević, V. Stojanović, and D. Kostić, Construction and optimization of the seventh-order polynomial convolutional interpolation 2P kernel, in *11th International Conference Modern Trends in Science, FMNS-2025*, Book of Abstracts, Blagoevgrad, Bulgaria, pp. 211–212, 2025.

Zoran Milivojević obtained BSc, MSc and PhD degrees at the Faculty of Electronic Engineering, University of Niš, Serbia. He is a full professor at MB University in Belgrade, at the Department of Information Technologies, and Academy of Technical-Educational Vocational Studies - at the Department of Information Technologies, Niš, Serbia. He is a regular member of the Engineering Academy of Serbia, Department of Electrical and Computer Engineering. His primary research interests are digital signal processing in the field of image and audio signal processing: algorithms and applications. He is the author and co-author of more than 300 papers published in national and international journals (over 30 journals indexed by Thomson SCI/SCIE JCR), conference proceedings, as well as book chapters published by Springer.

Predrag Rajković Ph.D., is professor at the Department of Mathematics and Informatics, of Mechanical Engineering Faculty at the University of Niš in Serbia. He published over 160 scientific papers and 3 monographs mainly dealing with the mathematical disciplines: Numerical Analysis (Interpolation, Approximation, Numerical Integration), Quantum Calculus, Mathematical Programming, Optimization, Special Functions and Transforms. He has been on the editorial boards and reviewer of several respected international journals. He has been the visiting professor at University in Kassel (Germany), South East Technological University (Ireland), Malardalen University (Sweden) and Masaryk University (Czech). In his 40 years of teaching experience, he has published 4 textbooks. He was advisor of 2 doctoral dissertations and foreign examiner for more than 20. He had participated in 10 international and domestic projects and more than 50 conferences, often as a member of organizing and scientific committee.